ACS APPLIED MATERIALS & INTERFACES

Letter

www.acsami.org

Phospholipid Bilayer-Coated Aluminum Nanoparticles as an Effective Vaccine Adjuvant-Delivery System

Ting Wang,*[,†] Yuanyuan Zhen,[†] Xiaoyu Ma,[†] Biao Wei,[†] and Ning Wang*[,‡]

[†]School of Pharmacy, Anhui Medical University, 81 Plum Hill Road, Hefei, Anhui Province 230032, China

[‡]School of Medical Engineering, Hefei University of Technology, 193 Tun Brook Road, Hefei, Anhui Province 230009, China

Supporting Information

ABSTRACT: The *p*hospho*l*ipid bilayer-coated *a*luminum *n*anoparticles (PLANs), formed via chemisorption, were prepared by reverse ethanol injection-lyophilization (REIL) utilizing the phosphophilicity of aluminum. The anhydrous antigen-loaded PLANs obtained by REIL proved stable, satisfying using the controlled-temperature-chain instead of the integrated cold-chain for distribution, and could be rehydrated to reconstitute instantly an aqueous suspension of the antigen-PLANs, which were more readily taken up by antigen-presenting cells and, when given subcutaneously to mice, induced more robust antigen-specific humoral and cellular immunoresponses but less local inflammation than the antigen-alum. Thus, the PLANs are a useful vaccine adjuvant-delivery system with advantages over the widely used naked alum.

KEYWORDS: *antigen, chemisorption, immune response, lyophilization, nanoparticle*

Vaccination has proven to be the most cost-effective and the best prophylactic strategy against many diseases.[1] To develop effective vaccines, scientists usually need adjuvants, which are the ingredients that can enhance and even direct the adaptive immunoresponses toward a specific pathway to vaccine antigens, to be included in the products. This is especially true for subunit vaccines that contain only the essential antigens and lack other microbe components to fit the pathogen-associated molecular patterns (PAMPs) for mammal immune systems and, therefore, often induce very weak or moderate immunoresponses.[2,3] Several materials have now been recognized and further confirmed by the pre- and clinical trials as effective vaccine adjuvants, e.g. aluminum salts, the ligands to C-type lectin or toll-like receptors, and different kinds of particulate carriers such as emulsions, liposomes, and silica nanoparticles.[4,5] Aluminum salt, known as alum, such as aluminum hydroxide/phosphate, is the first vaccine adjuvant developed initially by Glenny and co-workers in the 1920s and has been safely used since in more than 80% of the vaccines that have ever entered markets.[6,7] Up to now, though billions of doses of alum-adjuvanted vaccines have been administered to humans, the exact mechanism of alum action on mammal immune systems remains unclear and is argued to involve several physicochemical and biological activities of alum.[8] Notably, recent investigations on the direct interaction between alum and immunocytes have uncovered many signaling details in the alum-involved immunoresponse process, with, unfortunately, some results at odds with each other.[9−11] Nevertheless, at present, it seems true that although it can hardly be taken up by immunocytes, the micron-sized conventional alum can enormously facilitate the cellular uptake of the adjuvanted vaccines by APCs, which, subsequently, will initiate the serial immunoresponses via a Th2 pathway to set up immunity.[11] Interestingly, in the past two decades the conventional alum has been explored to combine with other adjuvants, such as lipid A, and successfully formulated into a vaccine adjuvant-delivery system (VADS) against pathogens.[7,12] Also, recently it has been reported that after being engineered into nanoparticles, the alum can be readily phagocytosed by APCs, promoting simultaneously the cellular uptake and cross-presentation of the carried antigens enhancing humoral as well as cellular immunoresponses.[13,14]

Herein, to develop the alum-based VADSs that have also the ability to induce both humoral and cellular immunoresponses, the *p*hospho*l*ipid bilayer-coated *a*lum *n*anoparticles (PLANs) were prepared as an antigen carrier. First, the aluminum hydroxide nanoparticles (ANs) were synthesized by neutralization of aluminum chloride with ammonia in respective reverse microemulsions which contained Triton-X100/Igepal CO-520

Received: January 13, 2015
Accepted: March 17, 2015
Published: March 17, 2015

DOI: 10.1021/acsami.5b00348
ACS Appl. Mater. Interfaces 2015, 7, 6391−6396

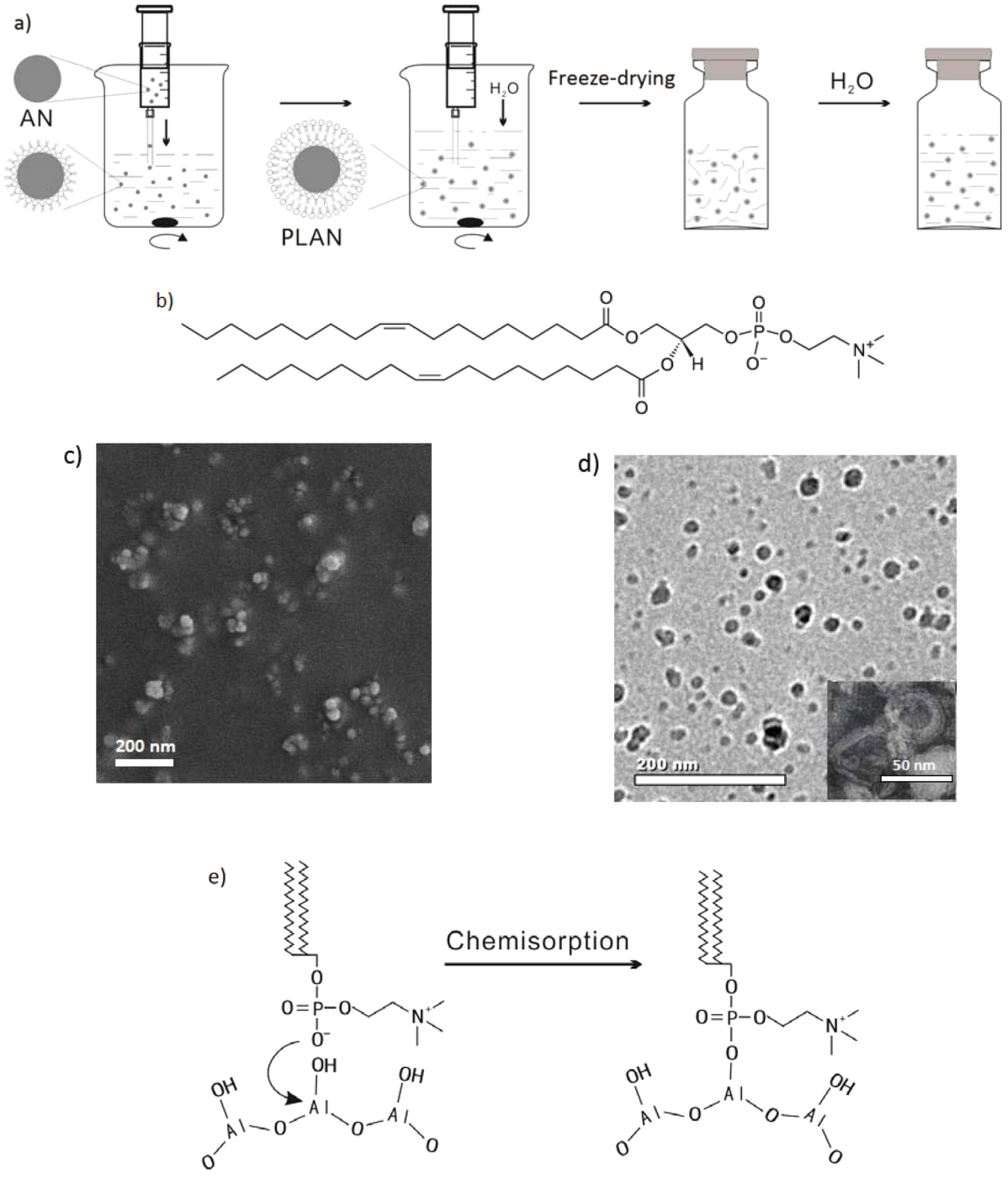

Figure 1. Features of the PLANs by REIL. (a) Schematic REIL process for preparing the PLANs. (b) Molecular structure of DOPC. (c) SEM of the dry precursor to the PLANs prepared by REIL. (d) Cryo-TEM of the PLANs with inserted negative staining TEM of the PLANs. (e) Process of chemisorption of DOPC by aluminum.

as both an emulsifier and the particle size controller.[15] Then, the PLANs were prepared by a simple procedure of reverse ethanol injection-lyophilization (REIL) method (Figure 1a) with DOPC (1,2-dioleoyl-*sn*-glycero-3-phosphocholine) as a coating material (Figure 1b). The prepared ANs had a controllable size of around 40 nm and zeta potential (ζ) of 50 mV (Table S1 in the Supporting Information), and they could be further engineered by REIL into the PLANs embedded in a dry product (Figure 1c), which could be hydrated to reconstitute instantly an aqueous suspension of the PLANs (DOPC/AN = 1:3, w/w) (Figure 1d) with a size of around 50 nm but ζ of 25 mV (Table S1). The X-ray diffraction patterns (Figure S1 in the Supporting Information) reveal that the aluminum hydroxide in the PLANs, ANs or AMs (alum microparticles) all had the rather low crystallinity, which may also contribute to enhancing the adjuvanticity of alum.[13] On the basis of the property of phosphophilicity (avidity for phosphate) of aluminum[16] (Figure S2) and the unique process of REIL, it is speculated that during preparation the ANs are first coated with a lipid monolayer in the ethanol/water (2:1, v/v) cosolvent and then a bilayer, when additional bulk water dominates the system to engender hydrophobic effects as a

DOI: 10.1021/acsami.5b00348
ACS Appl. Mater. Interfaces 2015, 7, 6391−6396

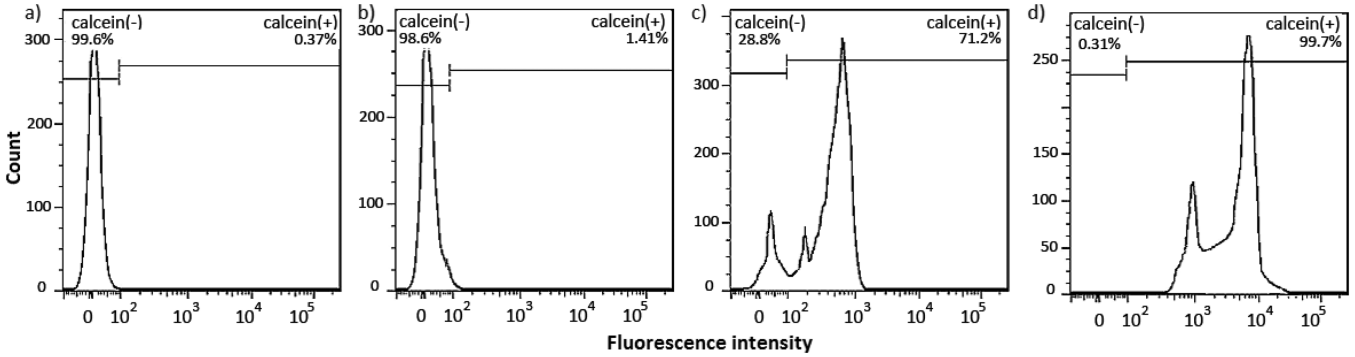

Figure 2. Flow cytometry assay of the uptake by BMDCs of different calcein-containing formulations (n = 3). The BMDCs (1×10^5) had been incubated in normal saline with (a) blank saline, (b) calcein-AMs, (c) calcein-ANs, and (d) calcein-PLANs. The percentage numbers in each panel indicate the fraction of the cells that had (right) or not (left) taken up calcein.

driving force on lipids (Figure 1a). FTIR spectroscopy of the lyophilized product shows a characteristic peak at ~1050 cm^{-1} (Figure S3 in the Supporting Information), which is assigned to be the framework vibrations of Al−O−P, a covalent linkage engendered as a result of a nucleophilic attack at the Al center by DOPC phosphate oxygen (Figure 1e),[17] a process often referred to as ligand exchange.[18] Thus, the ANs in the lyophilized products should be firmly coated with a phospholipid bilayer with the inner monolayer being associated via chemisorption. And this is also supported by the observation that the formation of the PLANs was insensitive at all to NaCl ion concentration (Table S1 in the Supporting Information).[17] Intriguingly, thanks to catching by just chemisorption some of the trace of free Al^{3+} ions in solution, the PLANs were positively charged with a ζ of 25 mV, engendering a cationic nanocarrier which is sometimes a desirable VADS against pathogens.[19] Obviously, during REIL, if only DOPC were surplus to forming the PLANs, would the empty large liposomes be created as a byproduct, which, thus, could be minimized through quantitatively controlling the amount of lipids needed. This is well-evidenced by the fact that when the DOPC/alum mass ratio was over 1:3, the size of the particles in the products increased remarkably (Figure S4 in the Supporting Information) as a result of formation of large liposomes from the surplus lipids. However, the excessive lipids might as well be used to prepare the novel VADS, because, when necessary, the empty liposomes can be easily removed from the PLANs by centrifugation based on density difference. Notably, when conventional ethanol injection method[20] was employed, only a few of the PLANs to be needed were gained, because numerous large liposomes associated with the ANs on their surfaces were preferentially formed (Figure S5 in the Supporting Information).

To evaluate the efficacy of the novel VADS, the OVA-PLANs (OVA/AN/DOPC = 1:18:5, w/w) with a size and ζ similar to those of the blank PLANs (Table S1 in the Supporting Information) were prepared by REIL for vaccination of mice. In contrast to the OVA in saline, the anhydrous OVA-PLAN precursors were rather stable and proved by SDS-PAGE able to maintain the antigen integrity during 4 days of storage at 40 °C (Figure S6 in the Supporting Information), allowing the vaccines to transport in the controlled temperature chain (CTC) instead of the integrated cold chain, which is now indispensably adhered to by most vaccines but is often unavailable in remote districts of less-developed countries.[21,22] As expected, because of the high stability and strong (chemi)adsorption of alum to phosphate-possessing OVA,[23] the antigen release from the PLANs was rather slow, and more than 95 and 60% of the loaded OVA were still associated with the carrier after 72 h incubation at 37 °C in saline and in sheep tissue fluid solution, respectively (Figure S7 in the Supporting Information). Thus, the PLANs may act as a good vaccine depot despite the fact that certain alum-associated antigens are eluted rapidly from the adjuvant when they are exposed to interstitial fluid.[24]

The in vitro cellular uptake was tested using the calcein/OVA-PLANs (calcein/alum = 1:90, w/w), -ANs, or -AMs. Calcein was used because it exhibits strong green fluorescence and is unable to enter cells without carriers to mediate it due to its impermeability to cell membranes;[25] moreover, it can well complex alum.[26] The fluorescent microscopy images (Figure S8 in the Supporting Information) indicate that although the calcein/OVA-PLANs and -ANs were both enormously taken up by mouse BMDCs, the calcein/OVA-AMs were rarely. Further investigation with flow cytometry unravel that both the fraction of the cells that had taken up calcein and the average amount of calcein taken up by each cell (as shown by the fluorescence intensity in Figure 2) were largest in BMDCs that had been incubated with the calcein/OVA-PLANs. Therefore, owing to the high compatibility as well as the electrostatic attraction between cell membranes and the positively charged lipid bilayer coatings, the agent-loaded PLANs can be more efficiently taken up by APCs than the naked ANs, which still favor the cellular uptake to contrast the AMs.

Also, the stored as well as the fresh OVA-PLANs were most effective in induction of the anti-OVA antibody production in s.c. vaccinated mice, as evidenced by the levels of antigen-specific IgG and IgA tested at different times (Figure 3a, b and Figure S9 in the Supporting Information), which also display that the immunity established by the PLANs was more durable than by other formulations (Figure 3a). Interestingly, all the mice received the alum-adjuvanted vaccines via s.c. route gained robust intestinal but not vaginal mucosal immunity (Figure 3b), which is usually established only through mucosal vaccination.[27] However, the mucosal immunity was less durable than other humoral immunity established simultaneously by the OVA-PLANs, since, in contrast to the antigen-specific IgG levels, the IgA levels in the same mice had already declined to below the significance in just 27 weeks after immunization (Figure 3c). Measurement of the levels of IgG1 and IgG2a subsets gives insight into the types of T helper cell immunoresponses. As shown in Figure 3d, the OVA-AMs

DOI: 10.1021/acsami.5b00348
ACS Appl. Mater. Interfaces 2015, 7, 6391−6396

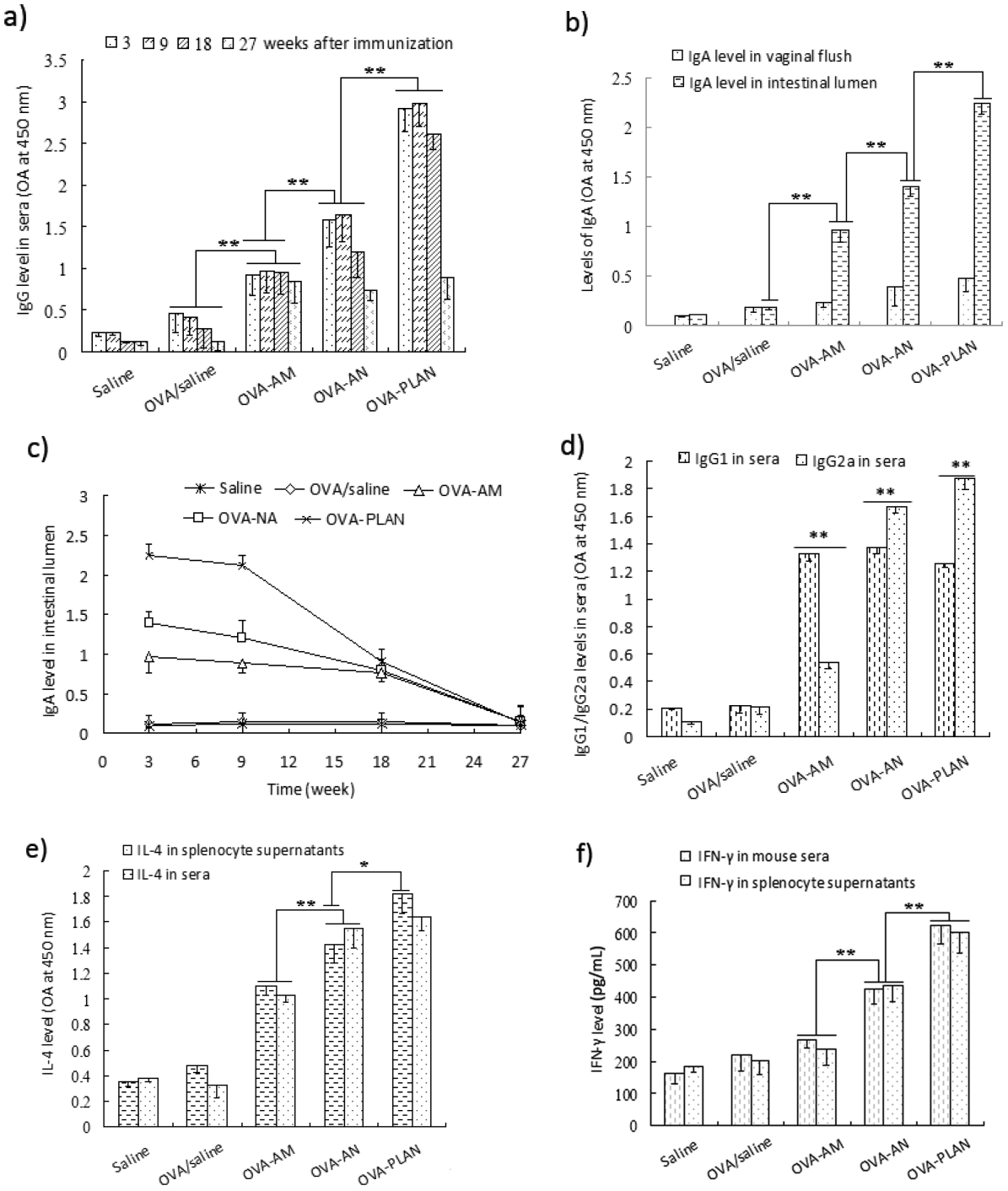

Figure 3. Immunoglobulin and cytokine assay of immunized mice (n = 6). (a) Levels of IgG in mouse sera (1:5000 dilution) detected at different time intervals after s.c. immunization. (b) Levels of IgA in mouse different tissue mucosa (1:500 and 1:50 dilution for intestinal and vaginal samples, respectively) detected 3 weeks after immunization. (c) Levels of IgA in mouse intestinal lumen at different time intervals after immunization. (d) Levels of IgG1 and IgG2a in mouse sera (1:200 dilution) detected 3 weeks after immunization. (e, f) Levels of IL-4 and IFN-γ in mouse sera (1:10 dilution) and splenocyte (1×10^5) cultures. (* p value <0.05, ** p value <0.01, in comparison to negative control).

significantly enhanced the anti-OVA IgG1 levels in treated mice, resulting in the highest IgG1/IgG2a ratio indicating a Th2-biased immunoresponse; by comparison, the PLAN or AN formulation remarkably increased IgG1 as well as IgG2a levels, leading to a more balanced Th1/Th2 response. These differential immunoresponses are further distinguished by the IL-4 and IFN-γ levels tested in treated mice sera as well as the culture media of the splenocytes that were isolated from treated mice and further stimulated with OVA. While IL-4 levels were elevated dramatically in all treated mice compared to the negative control (Figure 3e), the IFN-γ levels were only remarkably enhanced in the mice that received the OVA-ANs and, especially, the OVA-PLANs (Figure 3f). The flow cytometry assay of $CD4^+/CD8^+$ T cell subsets by figuring out the two phenotypes of the splenocytes in treated mice (Figure 4) shows that, by comparison to the negative control, while the percentage of $CD4^+$ T cells was remarkably increased in all mice treated the adjuvanted vaccines, the percentage of $CD8^+$ T

DOI: 10.1021/acsami.5b00348
ACS Appl. Mater. Interfaces 2015, 7, 6391−6396

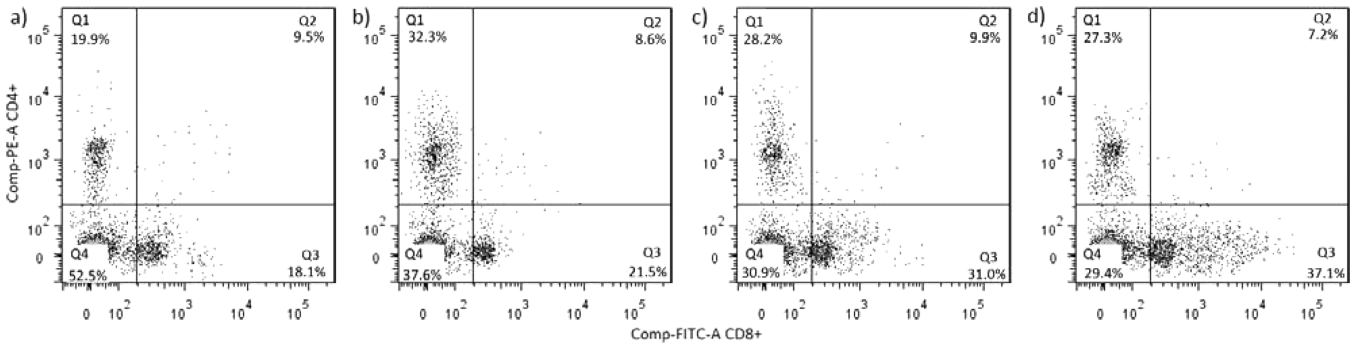

Figure 4. Flow cytometry assay of splenocytes (1×10^5) labeled with PE-anti-CD8$^+$ mAb and FITC-anti-CD4$^+$ mAb ($n = 6$). The splenocytes were from mice s.c. immunized with (a) normal saline, (b) OVA-MAs, (c) OVA-ANs, or (d) OVA-PLANs.

cells was increased significantly in the AN-treated mice and most significantly in the PLAN-treated mice. The MTT tests reveal also that the strongest splenocytes proliferation occurred in the mice that received the OVA-PLANs (Figure S10 in the Supporting Information). All these results suggest that the nanoparticulate alum, especially with the lipid bilayer coatings, has the ability to induce both humoral and cellular immunoresponses through being readily taken up by APCs to facilitate the cross-presentation of the loaded antigens.[28] The exact mechanism for this remains unknown now; however, it may possibly be that the PLANs efficiently deliver the loaded antigens not only into APCs but also to the organelle of autophagosomes in APCs, which will consequently process and cross-present the antigens through autophagy to T cells.[14] This autophagy pathway involved in the vaccine-induced immunoresponses has already been documented with a VADS of α-Al_2O_3 nanoparticles, which are just similar to the PLANs.[14]

To track the PLANs in vivo, the calcein/OVA-loaded particles were s.c. injected into the right forelimb lateral site of mice. The fluorescence microscopy of the histological sections indicates that, 16 h after the injection, the PLANs were remarkably accumulated in the axillary lymph node (Figure S11 in the Supporting Information), whereas the AMs as well as the ANs were rarely detected in the lymph nodes (data are not shown). The possible reason for this is that the naked alum in tissues may be rapidly neutralized via chemisorption by the affluent phosphate or proteins in interstitial fluids, impeding the interactions between APCs and particles preventing the subsequent proper cellular uptake; otherwise, the naked alum may disturb the cellular membranes of APCs[11] crippling migration ability of these lymph node-bound cells which may have be injured. Though the cellular membrane-disturbing phenomenon has been observed by the other group, the subsequent results and related mechanisms remain yet unclear.[11] Flow cytometry assay of the lymph node cells reveal that the agent-loaded PLANs were mainly taken up by DCs (Figure S12 in the Supporting Information), which might have been lingering at the injection site and, after readily picking up the vaccines, travel to the lymph nodes. The fact that only a small fraction of the PLANs was taken up by the macrophages indicates that, in contrast to the stealth nanocarriers,[29] the PLANs can hardly deliver the loaded agents from the injection site directly to the lymphocytes within lymph nodes.

Finally, the microscopes of the histological sections demonstrate that when intramuscularly given to mice neither the PLANs nor the ANs initiated the obvious inflammation in muscles with the injection, whereas the AMs elicited the severe inflammatory reactions, as indicated by the number of neutrophils accumulated in the injection sites (Figure S13 in the Supporting Information). Thus, the lipid coating can effectively improve the safety profile of alum.

In summary, the PLANs entrapping vaccine antigens were successfully prepared using REIL, which produced first a dry PLAN precursor applicable to the CTC, providing the possibility for wide vaccination in remote districts where the integrated cold chain is not available. The PLANs could induce a mixed Th1/Th2 immunoresponse to establish both humoral and cellular and even mucosal immunity to the loaded antigens. Moreover, possessing the liposome-like structure renders the PLANs some promising usage perspectives, e.g., the lymph node-targeting delivery may be achieved by surface modification and pegylation; the adjuvanticity may be further improved by incorporating other adjuvant materials; also, carrying the therapeutic genes or RNAs for treatment may be feasible by exploiting the phosphophilicity. Thus, the PLANs may be a safe multifunctional VADS or DDS against various diseases.

■ ASSOCIATED CONTENT

Supporting Information

Abbreviations, experimental section, characteristics of the PLANs, uptake of the PLANs by mouse BMDCs, splenocyte proliferation of the vaccinated mice, distribution of the PLANs in lymph node, uptake of the PLANs by different APCs in lymph node, local stimulatory effect. This material is available free of charge via the Internet at http://pubs.acs.org/.

■ AUTHOR INFORMATION

Corresponding Authors

*E-mail: twangcn@hotmail.com.
*E-mail: nwangcn@163.com.

Notes

The authors declare no competing financial interest.

■ ACKNOWLEDGMENTS

The authors acknowledge that this work was financially supported by National Natural Science Foundation of China (Grant 81273452), the Elite Faculty S&R Project Startup Fund of AMU Grant XJ201206), and also by the Fundamental Research Funds for the Central Universities (HUT).

■ REFERENCES

(1) Ozawa, S.; Mirelman, A.; Stack, M. L.; Walker, D. G.; Levine, O. S. Cost-Effectiveness and Economic Benefits of Vaccines in Low- and Middle-Income Countries: a Systematic Review. *Vaccine* **2012**, *31*, 96−108.

DOI: 10.1021/acsami.5b00348
ACS Appl. Mater. Interfaces 2015, 7, 6391−6396

(2) De Gregorio, E.; Rappuoli, R. From Empiricism to Rational Design: a Personal Perspective of the Evolution of Vaccine Development. *Nat. Rev. Immunol.* **2014**, *14*, 505−514.
(3) Moyle, P. M.; Toth, I. Modern Subunit Vaccines: Development, Components, and Research Opportunities. *ChemMedChem* **2013**, *8*, 360−376.
(4) Reed, S. G.; Orr, M. T.; Fox, C. B. Key Roles of Adjuvants in Modern Vaccines. *Nat. Med.* **2013**, *19*, 1597−1608.
(5) Pearton, M.; Kang, S. M.; Song, J. M.; Kim, Y. C.; Quan, F. S.; Anstey, A.; Ivory, M.; Prausnitz, M. R.; Compans, R. W.; Birchall, J. C. Influenza Virus-Like Particles Coated onto Microneedles Can Elicit Stimulatory Effects on Langerhans Cells in Human Skin. *Vaccine* **2010**, *28*, 6104−6113.
(6) Glenny, A.; Pope, C.; Waddington, H.; Wallace, U. The Antigenic Value of Toxoid Precipitated by Potassium Alum. *J. Pathol.* **1926**, *29*, 31−40.
(7) Garcon, N.; Chomez, P.; Van Mechelen, M. Glaxosmithkline Adjuvant Systems in Vaccines: Concepts, Achievements and Perspectives. *Expert Rev. Vaccines* **2007**, *6*, 723−739.
(8) Exley, C.; Siesjo, P.; Eriksson, H. The Immunobiology of Aluminium Adjuvants: How Do They Really Work? *Trends Immunol.* **2010**, *31*, 103−109.
(9) Hornung, V.; Bauernfeind, F.; Halle, A.; Samstad, E. O.; Kono, H.; Rock, K. L.; Fitzgerald, K. A.; Latz, E. Silica Crystals and Aluminum Salts Activate the NALP3 Inflammasome through Phagosomal Destabilization. *Nat. Immunol.* **2008**, *9*, 847−856.
(10) Leslie, M. Solution to Vaccine Mystery Starts to Crystallize. *Science* **2013**, *341*, 26−27.
(11) Flach, T. L.; Ng, G.; Hari, A.; Desrosiers, M. D.; Zhang, P.; Ward, S. M.; Seamone, M. E.; Vilaysane, A.; Mucsi, A. D.; Fong, Y.; Prenner, E.; Ling, C. C.; Tschopp, J.; Muruve, D. A.; Amrein, M. W.; Shi, Y. Alum Interaction with Dendritic Cell Membrane Lipids Is Essential for Its Adjuvanticity. *Nat. Med.* **2011**, *17*, 479−487.
(12) Didierlaurent, A. M.; Morel, S.; Lockman, L.; Giannini, S. L.; Bisteau, M.; Carlsen, H.; Kielland, A.; Vosters, O.; Vanderheyde, N.; Schiavetti, F.; Larocque, D.; Van Mechelen, M.; Garcon, N. AS04, an Aluminum Salt- and TLR4 Agonist-Based Adjuvant System, Induces a Transient Localized Innate Immune Response Leading to Enhanced Adaptive Immunity. *J. Immunol.* **2009**, *183*, 6186−6197.
(13) Sun, B.; Ji, Z.; Liao, Y. P.; Wang, M.; Wang, X.; Dong, J.; Chang, C. H.; Li, R.; Zhang, H.; Nel, A. E.; Xia, T. Engineering an Effective Immune Adjuvant by Designed Control of Shape and Crystallinity of Aluminum Oxyhydroxide Nanoparticles. *ACS Nano* **2013**, *7*, 10834−10849.
(14) Li, H.; Li, Y.; Jiao, J.; Hu, H. M. Alpha-Alumina Nanoparticles Induce Efficient Autophagy-Dependent Cross-Presentation and Potent Antitumour Response. *Nat. Nanotechnol.* **2011**, *6*, 645−650.
(15) Tseng, Y. C.; Xu, Z.; Guley, K.; Yuan, H.; Huang, L. Lipid-Calcium Phosphate Nanoparticles for Delivery to the Lymphatic System and SPECT/CT Imaging of Lymph Node Metastases. *Biomaterials* **2014**, *35*, 4688−4698.
(16) Zhao, Q.; Sitrin, R. Surface Phosphophilicity of Aluminum-Containing Adjuvants Probed by Their Efficiency for Catalyzing the P–O Bond Cleavage with Chromogenic and Fluorogenic Substrates. *Anal. Biochem.* **2001**, *295*, 76−81.
(17) Wang, F.; Liu, J. Liposome Supported Metal Oxide Nanoparticles: Interaction Mechanism, Light Controlled Content Release, and Intracellular Delivery. *Small* **2014**, *10*, 3927−3931.
(18) Hansen, B.; Belfast, M.; Soung, G.; Song, L.; Egan, P. M.; Capen, R.; Hogenesch, H.; Mancinelli, R.; Hem, S. L. Effect of the Strength of Adsorption of Hepatitis B Surface Antigen to Aluminum Hydroxide Adjuvant on the Immune Response. *Vaccine* **2009**, *27*, 888−892.
(19) Even-Or, O.; Joseph, A.; Itskovitz-Cooper, N.; Samira, S.; Rochlin, E.; Eliyahu, H.; Goldwaser, I.; Balasingam, S.; Mann, A. J.; Lambkin-Williams, R.; Kedar, E.; Barenholz, Y. A New Intranasal Influenza Vaccine Based on a Novel Polycationic Lipid-Ceramide Carbamoyl-Spermine (CCS). II. Studies in Mice and Ferrets and Mechanism of Adjuvanticity. *Vaccine* **2011**, *29*, 2474−2486.
(20) Gentine, P.; Bourel-Bonnet, L.; Frisch, B. Modified and Derived Ethanol Injection toward Liposomes: Development of the Process. *J. Liposome Res.* **2013**, *23*, 11−19.
(21) Zipursky, S.; Djingarey, M. H.; Lodjo, J. C.; Olodo, L.; Tiendrebeogo, S.; Ronveaux, O. Benefits of Using Vaccines out of the Cold Chain: Delivering Meningitis A Vaccine in a Controlled Temperature Chain During the Mass Immunization Campaign in Benin. *Vaccine* **2014**, *32*, 1431−1435.
(22) Wang, N.; Wang, T.; Zhang, M.; Chen, R.; Niu, R.; Deng, Y. Mannose Derivative and Lipid A Dually Decorated Cationic Liposomes as an Effective Cold Chain Free Oral Mucosal Vaccine Adjuvant-Delivery System. *Eur. J. Pharm. Biopharm.* **2014**, *88*, 194−206.
(23) Zarif, L. Drug Delivery by Lipid Cochleates. *Methods Enzymol.* **2005**, *391*, 314−329.
(24) Iyer, S.; Hogenesch, H.; Hem, S. L. Relationship between the Degree of Antigen Adsorption to Aluminum Hydroxide Adjuvant in Interstitial Fluid and Antibody Production. *Vaccine* **2003**, *21*, 1219−1223.
(25) Kendall, D. A.; Macdonald, R. C. A Fluorescence Assay to Monitor Vesicle Fusion and Lysis. *J. Biol. Chem.* **1982**, *257*, 13892−13895.
(26) Li, H. B.; Chen, F. A Highly Sensitive Fluorimetric Method for the Determination of Fluoride in Biological Material with $Al3^{+}$-Calcein Complex. *Fresenius J. Anal. Chem.* **2000**, *368*, 501−504.
(27) Neutra, M. R.; Kozlowski, P. A. Mucosal Vaccines: the Promise and the Challenge. *Nat. Rev. Immunol.* **2006**, *6*, 148−158.
(28) Norman, J. J.; Arya, J. M.; Mcclain, M. A.; Frew, P. M.; Meltzer, M. I.; Prausnitz, M. R. Microneedle Patches: Usability and Acceptability for Self-Vaccination Against Influenza. *Vaccine* **2014**, *32*, 1856−1862.
(29) Muraoka, D.; Harada, N.; Hayashi, T.; Tahara, Y.; Momose, F.; Sawada, S.; Mukai, S. A.; Akiyoshi, K.; Shiku, H. Nanogel-Based Immunologically Stealth Vaccine Targets Macrophages in the Medulla of Lymph Node and Induces Potent Antitumor Immunity. *ACS Nano* **2014**, *8*, 9209−9218.

DOI: 10.1021/acsami.5b00348
ACS Appl. Mater. Interfaces 2015, 7, 6391−6396